Physics of Fluids

RESEARCH ARTICLE | JULY 01 1987

Magnetohydrodynamic stability of hot-electron stabilized tandem mirrors

D. Dobrott; S. Kendrick; Robert P. Freis; Bruce I. Cohen

Check for updates

Phys. Fluids 30, 2149–2154 (1987)
https://doi.org/10.1063/1.866149

View Online
Export Citation

Articles You May Be Interested In

Interchange, rotational, and ballooning stability of long-thin axisymmetric systems with finite-orbit effects

Phys. Fluids (May 1986)

Finite Larmor radius stabilization of ballooning modes in an axisymmetric tandem mirror

Phys. Fluids (December 1981)

Tandem mirror trapped particle instability driven by axial shear in $E \times B$ rotation

Phys. Fluids (May 1986)

03 October 2025 23:10:05

AIP Publishing

Magnetohydrodynamic stability of hot-electron stabilized tandem mirrors

D. Dobrott and S. Kendrick
Science Applications International Corporation, La Jolla, California 92037
Robert P. Freis and Bruce I. Cohen
Lawrence Livermore National Laboratory, University of California, Livermore, California 94550

(Received 29 December 1986; accepted 26 March 1987)

The influence of energetic electron rings, or disks, on the magnetohydrodynamic stability of an axisymmetric tandem mirror configuration is studied. Linear stability equations describing interchange and ballooning modes are solved both analytically and numerically using a two-dimensional stability code for axisymmetric mirrors. Finite-ion-Larmor-radius effects and the presence of a lateral wall are included in the calculations. Stable configurations can be obtained with either sufficiently high hot-electron pressure or with sufficiently high center-cell pressure if a lateral conducting wall is close enough to the plasma. In particular, hot electrons might be used to stabilize transiently the plasma during buildup to a high-beta, wall-stabilized configuration.

I. INTRODUCTION

Most current tandem mirror configurations rely on minimum-B end cells to provide overall magnetohydrodynamic stability.[1,2] Quadrupole magnetic coils are typically used in the end cells, which ensures that the end cells are absolute minimum-B configurations when standing alone. In a tandem mirror, the center cell is axisymmetric and is only neutrally stable. When connected to stabilizing end cells, average minimum-B stability can be achieved if the requisite pressure-weighted curvature integral is favorable. As the plasma pressure is increased, ballooning modes can exploit regions that have unfavorable magnetic curvature, e.g., in the transition regions linking the center cell to the end cells.[2,3] With the inclusion of finite-ion-Larmor-radius (FLR) effects, analysis indicates that low-m (m is the azimuthal mode number) interchange and ballooning modes are the most dangerous and set the pressure limits for stability.[3]

The complexity of quadrupole magnetic structures significantly increases the capital cost of proposed reactor configurations. Furthermore, radial transport is likely to be much worse because of the departure of the equilibrium from axisymmetry.[4] These factors motivate consideration of completely axisymmetric systems. A number of mechanisms have been suggested to provide magnetohydrodynamic (MHD) stability in axisymmetric configurations.[5–10] Partial stabilization by line tying has been investigated theoretically and experimentally.[5] Complete MHD stability can be achieved with the combination of finite-ion-Larmor-radius effects and either a low pressure plasma in contact with a lateral wall[6] or a high pressure plasma separated by a thin vacuum region from the wall.[7,8] An energetic electron ring or disk can dig a magnetic well for the plasma, which is stabilizing if the energetic electrons are rigid with respect to the MHD perturbations.[9,10] In principle, axisymmetric radio-frequency wave stabilization of MHD modes is possible if an $m = 0$ launching scheme is used.[11]

Several aspects of the stability of axisymmetric tandem mirrors have been investigated previously.[10,12] We restrict our attention here to the study of MHD stability with finite-ion-Larmor-radius effects in the presence of both energetic electrons and a lateral wall. We assume that the configurations are strictly axisymmetric and long-thin.[12] We analytically derive a stability criterion for $m = 1$ rigid ballooning-interchange modes with a nearby wall and stabilizing hot electrons. We then relax the assumptions of rigidity and a nearby wall to investigate numerically the MHD stability more generally with the FLORA stability code.[12]

We find that a simple axisymmetric tandem mirror can be rendered stable by the combination of a rigid electron ring and a lateral wall for modest ring betas, $\beta_{\perp e} \geqslant 0.05$ ($\beta_{\perp e}$ is the ratio of the ring pressure to the local vacuum magnetic field energy density), and a center-cell beta value $\beta_{\perp c} = 0.4$. We also find that with $\beta_{\perp e} = 0.02$, the plasma is stable for $\beta_{\perp c} \geqslant 0.8$ and a 10% gap in radius between the edge of the center-cell plasma and the wall. Furthermore, our results indicate that the plasma is stable at finite values of $\beta_{\perp e}$ and sufficiently small $\beta_{\perp c}$. The plasma can be destabilized by increasing $\beta_{\perp c}$ and is eventually returned to stability at large values of $\beta_{\perp c}$ approaching unity if the lateral wall is nearby. Sufficiently large values of $\beta_{\perp e}$ can stabilize the plasma independent of the value of $\beta_{\perp c}$ within the constraints set by the mirror mode and the paraxial approximation.[12] A high-beta, wall-stabilized axisymmetric configuration is very attractive as a potential fusion device. The results presented here suggest building up to such a state through lower beta equilibria that are stabilized by hot electrons.

Our study of hot-electron stabilized axisymmetric tandem mirrors is by no means complete. We have assumed that the hot-electron ring is perfectly rigid with respect to perturbation and that the MHD displacement is incompressible. These assumptions should be relaxed.[9,10] When perturbations of the hot-electron plasma are taken into account, new modes of instability can occur: for example, the hot-electron interchange[13] and the unstable coupling of precessional and Alfvén waves.[14,15] In principle, stability with respect to these modes ought to constrain the parameter space available to us in trying to stabilize low-frequency ballooning-interchange

03 October 2025 23:10:05

modes. However, a detailed parametric study incorporating these constraints is beyond the scope of the present study, whose modest goal is to demonstrate the combined stabilizing effects of FLR, a nearby lateral wall, and hot electrons on low-frequency MHD modes. In what follows, we present a paraxial theory of ballooning-interchange modes, the results of analytical and numerical stability calculations, and a brief discussion.

II. LINEAR STABILITY THEORY

The paraxial theory of ballooning-interchange stability in axisymmetric mirror configurations with hot rigid electrons has been presented previously in Refs. 10 and 12. Here we will summarize the formulation of Ref. 12, which included FLR effects. The equations describing paraxial equilibria are perpendicular pressure balance

$$\frac{\partial}{\partial\psi}\left(\frac{B^2}{2}+p_{\perp p}+p_{\perp e}\right)=0 \tag{1}$$

and parallel pressure balance

$$\hat{b}\cdot\nabla(B^2/2+p_{\perp p}+p_{\perp e}) - B\cdot\nabla[(B^2+p_{\perp p}+p_{\perp e}-p_{\|p}-p_{\|e})/B]=0, \tag{2}$$

where ψ is the magnetic flux, B is the magnetic field, $p_{\perp p}$ and $p_{\|p}$ are the perpendicular and parallel components of the plasma pressure tensor, $p_{\perp e}$ and $p_{\|e}$ are the hot-electron-ring pressure tensor components, and the equations are cast in rationalized emu. Both the inverse aspect ratio of radial to axial length scales and the Larmor radius over the radial scale length are assumed small.

In Ref. 12, equations of motion for an incompressible, low-frequency, transverse, MHD displacement were derived based on a Lagrangian analysis. In the limit that the hot-electron beta is finite, but that its density is negligible so that charge uncovering that could be caused by the plasma cannot occur, the radial component of the linearized fluid displacement ξ satisfies

$$\begin{aligned}&\frac{\partial}{\partial\psi}\left(\rho Tr^4B\frac{\partial}{\partial\psi}\xi\right)\\&+(1-m^2)\rho\frac{T}{B}\xi+r^2\xi\frac{\partial}{\partial\psi}(\rho\omega^2)\\&-m^2r_{zz}r\xi\frac{\partial}{\partial\psi}(p_{\perp p}+p_{\|p})+m^2\frac{r^2}{B}\frac{\partial p_{\perp e}}{\partial\psi}\frac{\partial p_{\perp p}}{\partial\psi}\\&-m^2rB\frac{\partial}{\partial z}\left(\frac{Q}{r^2B^3}\frac{\partial}{\partial z}(rB\xi)\right)\\&+r\frac{\partial}{\partial\psi}\left\{\frac{B\partial}{\partial z}\left[\frac{Qr^2}{B}\frac{\partial}{\partial z}\left(B\frac{\partial}{\partial\psi}r\xi\right)\right]\right\}=0,\end{aligned} \tag{3}$$

where $Q=B_\perp^2+p_{\perp p}-p_{\|p}$, $\rho T=\rho\omega^2-m\omega\mathscr{X}-m^2\mathscr{Y}$, $(\partial/\partial t)=i\omega$, ρ is the mass density, r_{zz} is the normal curvature, and the FLR coefficients are

$$\mathscr{X}=2\rho\phi_\psi-(MB^2)_\psi/2B, \tag{4a}$$

$$\mathscr{Y}=-\rho\phi_\psi^2+(MB^2)_\psi(\phi_\psi/2B)-K_\psi B_\psi/B, \tag{4b}$$

where

$$M=-\sum_s n_s m_s^2\frac{\langle v_\perp^2\rangle_s}{q_sB}, \tag{5a}$$

$$K=\sum_s n_s m_s^3\frac{\langle v_\perp^4\rangle_s}{8q_s^2}, \tag{5b}$$

ϕ is the ambipolar potential, q_s is the species charge, n_s is the species number density, m_s is the species mass, and the brackets indicate an average over the distribution function. The fifth term in Eq. (3) contains the stabilizing magnetic well-digging effects of the hot rigid electrons.[9,10,12] The modes described are very low in frequency so that drift resonances cannot occur.

For a rotating isothermal Maxwellian plasma,

$$\mathscr{X}=\sum_s\rho_s(2\Omega_E+\Omega_{\nabla B}+\Omega^*)_s, \tag{6a}$$

and

$$\mathscr{Y}=-\sum_s\rho_s(\Omega_E+\Omega_{\nabla B})_s(\Omega_E+\Omega^*)_s, \tag{6b}$$

where

$$\Omega_E=\frac{\partial\phi}{\partial\psi}, \tag{7a}$$

$$\Omega^*=(e_sn_s)^{-1}\frac{\partial p_{\perp s}}{\partial\psi}, \tag{7b}$$

$$\Omega_{\nabla B}=(e_sn_s)^{-1}p_{\perp s}\frac{\partial\ln B}{\partial\psi} \tag{7c}$$

are the azimuthal $\mathbf{E}\times\mathbf{B}$, diamagnetic, and ∇B angular drift velocities.

The specification of the normal mode problem is completed with a statement of the boundary conditions on ξ. At some maximal flux surface corresponding to a conducting wall at $\psi=\psi_w$,

$$\xi=0, \tag{8a}$$

and for either an insulated free-end boundary,

$$\frac{\partial}{\partial z}(rB\xi)=0, \tag{8b}$$

or a line-tied boundary,

$$\xi=0, \tag{8c}$$

at $z=\pm L$, the location of the axial end plates. We will *not* consider line-tied boundary conditions here.

We now specialize to the consideration of the $m=1$ rigid mode. If the plasma is rotationally stable, then $m=1$ rigid modes are the most unstable MHD modes in the presence of strong FLR effects.[2,3,8,12] For convenience, we define

$$\beta_\perp\equiv 2p_{\perp p}/B_v^2, \tag{9a}$$

$$p\equiv(p_{\perp p}+p_{\|p})/2, \tag{9b}$$

$$\eta^2\equiv B_v/B=(1-\beta_\perp)^{-1/2}, \tag{9c}$$

$$\tilde{\phi}\equiv B^{1/2}\xi, \tag{9d}$$

$$\Lambda\equiv(R_w^2+R^2)/(R_w^2-R^2), \tag{9e}$$

where B_v is the vacuum magnetic field, R_w is the wall radius, and R is the plasma radius. If FLR effects are strong, then ρT is large and ξ is rigid to lowest order as a consequence of Eq. (3). Thus $\xi\approx\xi(z)$ and following Ref. 8 Eq. (3) becomes

03 October 2025 23:10:05

$$[\Lambda(\eta^2\tilde{\phi})']' + \frac{1}{\eta^2}\left(\frac{Q\tilde{\phi}'}{B^2}\right)' + \left(\frac{\rho\omega^2}{B_v^2} - \frac{2pR''}{B_v^2 R} + \frac{p_{\perp p}}{B_v^2 B}\frac{\partial p_{\perp e}}{\partial\psi}\right)\tilde{\phi} = 0, \quad (10)$$

where the primes denote partial derivatives with respect to z and a sharp-boundary pressure profile has been assumed. Equation (10) extends the result of Ref. 8 to include the potentially stabilizing well-digging effects of hot electrons in the last term to reduce the destabilizing effects of the curvature drive term containing R''. It is important to keep in mind that the hot electrons also contribute to the equilibrium pressure balance and can make the curvature locally more negative.

With the wall right on the plasma, $\Lambda \gg 1$ and $\eta^2\tilde{\phi} = 1 + \mathcal{O}(\Lambda^{-1})$. To obtain a dispersion relation, one integrates Eq. (10) from $z = -L$ to $z = L$ using the free-end boundary condition Eq. (8b), which leads to $\tilde{\phi}' = 0$ at $z = \pm L$. To lowest order in $\Lambda^{-1} \ll 1$, the eigenfrequency is given by

$$\omega_0^2 \int_{-L}^{L} dz \frac{\rho}{B_v^2} = \int_{-L}^{L} dz \left[\frac{2pR_v''}{B_v^2 R_v} + \frac{1}{8}\left(\frac{\beta_\perp'}{1-\beta_\perp}\right)^2 \times\left(1 - \frac{p}{B_v^2}\right) - \frac{\beta_\perp \partial p_{\perp e}/\partial\psi}{2B_v(1-\beta_\perp)^{1/2}}\right], \quad (11)$$

where $R_v = R/\eta$. The first term in the square bracket is the curvature drive, the second is positive definite ($Q > 0$) and demonstrates the stabilizing influence of finite pressure with the wall on the plasma, and the third term is the hot-electron well-digging contribution.

With a remote wall $\Lambda \sim 1$, one must employ other means to solve the balloon equation [Eq. (10)]. In Ref. 8, the substitution $\Phi = \eta\tilde{\phi}(z)$ was made, and a Sturm–Liouville equation for Φ was obtained from Eq. (10) with boundary conditions $\Phi' = \tilde{\phi}' = 0$ at $z \pm L$ ($\eta = 1$ near $z = \pm L$). A quadratic form was then constructed, and the choice of a flute trial function ($\Phi = 1$) led to a dispersion relation. The identical procedure here gives

$$\omega^2 \int_{-L}^{L} dz \frac{\rho}{BB_v} = \int_{-L}^{L} dz \left[\frac{2pR_v''}{BB_v R_v} + (\Lambda - 1)\eta^2 - \frac{\beta_\perp \partial p_{\perp e}/\partial\psi}{2B_v(1-\beta_\perp)}\right] \quad (12)$$

with the addition of the hot-electron well-digging contribution.

The important results of this section are contained in Eqs. (11) and (12), which demonstrate the combined effects of wall position and hot electrons on stability. With the wall right on the plasma surface, the second term on the right side of Eq. (11) can completely stabilize the plasma if $\beta_\perp$ and $\beta_\perp'$ are sufficiently large. If high-beta wall stabilization is insufficient, e.g., if $\beta_\perp$ or $\beta_\perp'$ is too small, then hot electrons can assist in stabilizing the plasma if $\partial p_{\perp e}/\partial\psi < 0$. With a distant wall, $(\Lambda - 1) \ll 1$, wall stabilization becomes very weak. The hot-electron well-digging term is unaffected by moving the lateral wall. LoDestro has generalized the wall-stabilization analysis of Ref. 8 to the case of diffuse pressure profiles.[16]

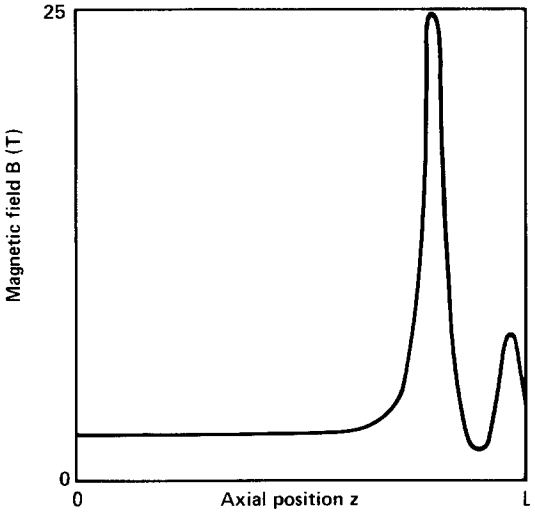

FIG. 1. Equilibrium magnetic field profile for a model long-thin axisymmetric tandem mirror.

III. NUMERICAL CALCULATIONS

We have made a quantitative evaluation of tandem mirror MHD stability with hot rigid electrons in the FLORA stability code.[12] A detailed description of the code's formulation and computational characteristics is given in Ref. 12. FLORA first calculates a self-consistent finite-beta paraxial equilibrium with model pressure profiles that satisfy Eqs. (1) and (2). The stability equation Eq. (3) is then solved as an initial-value problem with implicit finite-differencing techniques and FLR coefficients satisfying Eqs. (6) and (7). We used spatial meshes here that were more refined than those described in Ref. 12: 150 axial (z) grid points and 50 radial (ψ) grid points. Typical problems required 1600 time steps to determine clean growth rates, which correspond to approximately an hour of CRAY-2 computer time for each problem.

A simple tandem mirror equilibrium with hot electrons in the end cells is exhibited in Figs. 1–4. The flute-averaged, infinite-m, squared MHD growth rate γ_{mhd}^2 omits FLR ef-

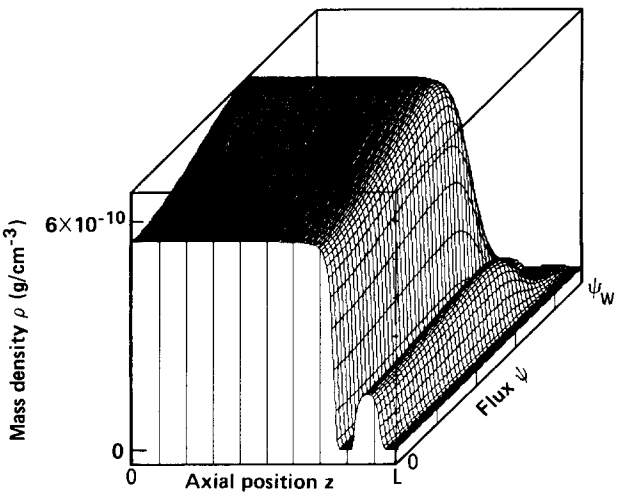

FIG. 2. Mass density profile for the model tandem mirror equilibrium of Fig. 1.

03 October 2025 23:10:05

fects, but it includes the influence of the hot electrons and gives valuable insight on the underlying MHD drive (Fig. 4). In the cases reviewed here, there was no electric potential and, hence, no rotational destabilization. Furthermore, the core-plasma radial pressure profile was slightly hollow, which enhanced its MHD stability. However, the core-plasma, flute-averaged, pressure-weighted curvature near the plasma surface was sufficiently negative to destabilize significantly these configurations in the absence of hot electrons and nearby conducting walls.

An important consideration in our stability calculations was the relative strength of the FLR coefficients. When the

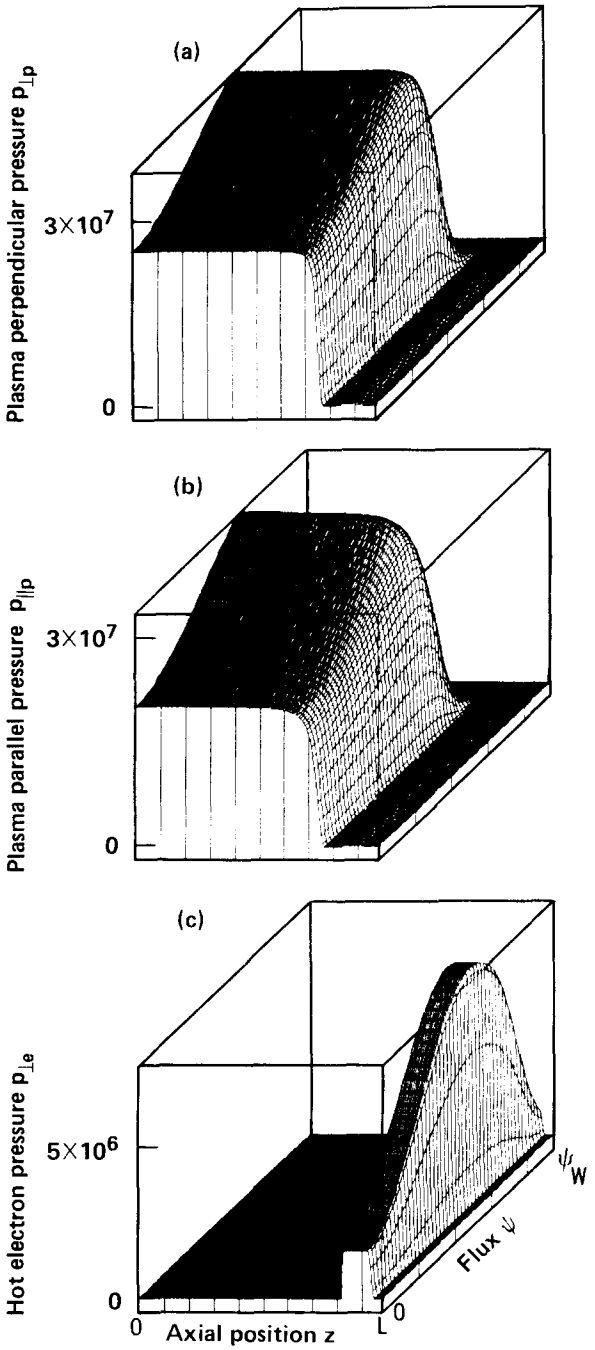

FIG. 3. Pressure profiles in the cgs system of units for the model tandem mirror equilibrium of Fig. 1: (a) plasma perpendicular pressure profile with peak beta value $\beta_{\perp c} = 0.9$, (b) plasma parallel pressure profile, and (c) hot-electron perpendicular pressure profile with peak beta value $\beta_{\perp e} = 0.1$.

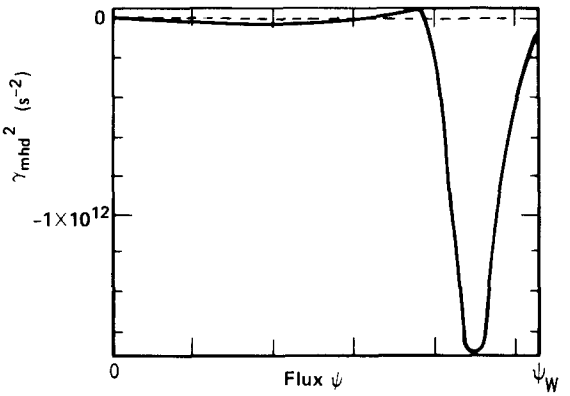

FIG. 4. The flute-averaged, infinite-m, squared MHD growth rate as a function of flux including the effects pressure-weighted curvature and hot-electron well digging for $\beta_{\perp c} = 0.8$ and $\beta_{\perp e} = 0.1$ peak values and other equilibrium characteristics as pictured in Figs. 1–3.

FLR coefficients were artificially reduced, the unstable $m = 1$ normal modes were less rigid with respect to their ψ variation and less susceptible to stabilization by either a nearby lateral wall at high beta or by hot-electron well digging at the plasma surface. Of course, accompanying the increased values of the FLR coefficients were higher oscillation frequencies ($\mathrm{Re}\,\omega$) for the normal modes. This increased the stiffness of the computational problem.[12]

The principal results of our numerical calculations are presented in Figs. 5 and 6. In the series of computer calculations exhibited, there was a center-cell plasma with density 2×10^{14} cm^{-3} and pressure that varied from case to case. There was a magnetically trapped plasma in the end cells whose density was fixed at 3×10^{13} cm^{-3} and whose peak $\beta_{\perp p}$ was 5×10^{-2}. The plasma in the end cell marginally satisfied the Nelson–Van Dam–Lee criterion,[17] $\beta_{\perp p} < \mathcal{O}(2Rr_{zz})$. The wall radius R_w in the center cell was fixed at a value $R_w = 42.4$ cm, and the relative plasma pressure at the lateral wall compared to its value on axis was fixed at $p_{\perp w}/p_{\perp o} = 1.2\times10^{-3}$. Cutting off the tail of the pressure profile near the wall and, hence, removing the FLR effects that extended to the wall had no effect on the linear stability calculations described here. This contrasts with

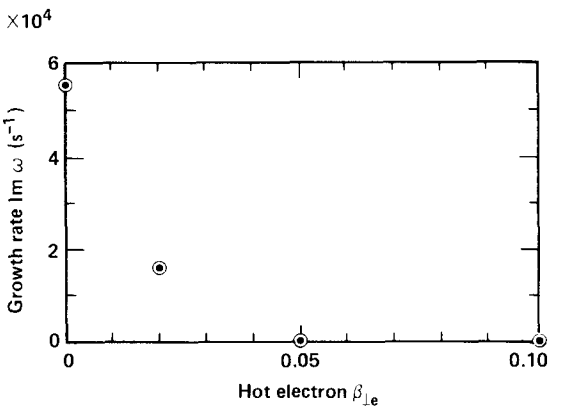

FIG. 5. Growth rates Im ω for $m = 1$ ballooning-interchange modes calculated in FLORA as a function of the hot-electron beta $\beta_{\perp e}$ with $\beta_{\perp c} = 0.4$, $R_p = 37.4$ cm, and $R_w = 42.4$ cm in the center cell.

03 October 2025 23:10:05

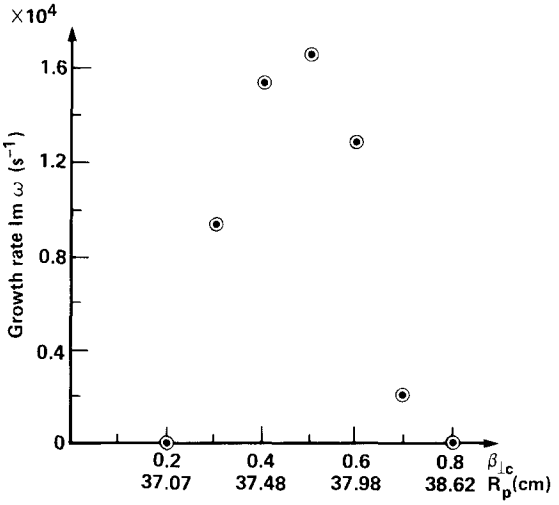

FIG. 6. Growth rates Im ω for $m = 1$ ballooning-interchange modes calculated in FLORA as a function of $\beta_{\perp c}$ with $\beta_{\perp e} = 0.02$ and $R_w = 42.4$ cm. The center-cell plasma radius R_p swells with increasing $\beta_{\perp c}$.

situations where stability is afforded by sufficiently strong FLR effects extending to a lateral wall where $\xi = 0$.[6,12]

The results of Fig. 5 indicate that a plasma with $\beta_{\perp c} = 0.4$ in the center cell and a fixed plasma radius $R_p = 37.4$ cm$(R_w/R_p = 1.13)$ is unstable to an $m = 1$ mode with no hot electrons, is stabilized with increasing hot-electron ring pressure, and is completely stable for $\beta_{\perp e} \geqslant 0.05$. The value of R_p is defined by the radius at which plasma $p_{\perp p}$ profile falls to half its peak value if there is no dip in $p_{\perp p}$ on axis. With a ring beta of $\beta_{\perp e} = 0.02$, the plasma is stable to $m = 1$ MHD modes for $\beta_{\perp c} \leqslant 0.2$ and is unstable for larger $\beta_{\perp c}$ until high-beta wall stabilization is achieved for $\beta_{\perp c} \geqslant 0.8$ (Fig. 6). Here the wall radius ($R_w = 42.4$ cm) and the magnetic flux were fixed in the center cell, and the center-cell plasma radius swelled with $\beta_{\perp c}$ compressing the flux in the vacuum region. Other numerical calculations with FLORA lacking the grid resolution of the cases shown here indicated that the plasma could be stabilized for any value of $\beta_{\perp c}$ by increasing $\beta_{\perp e}$ and that the plasma was stabilized at high $\beta_{\perp c}$ with no hot electrons when the conducting wall was reasonably close to the plasma. Furthermore, we found cases where stability depended jointly on the FLR, hot-electron, and wall effects. When any one of these effects were removed or suppressed, instability ensued and the $m = 1$ modes were the most unstable (see Table I). The possibility of joint stabilization is suggested explicitly by Eq. (11).

TABLE I. Dependence of tandem mirror MHD stability on FLR, hot electrons, and wall position for peak beta values $\beta_{\perp c} = 0.55$ and $\beta_{\perp e} = 0.8$ or 0. The central cell plasma radius was 42 cm.

Wall position (R_w/R_p)	FLR	Hot electrons	m	Stability
8.1	Yes	Yes	1	Unstable
1.4	Yes	Yes	1	Stable
1.4	No	Yes	1	Unstable
1.4	Yes	No	1	Unstable
1.4	No	No	1	Unstable
1.4	Yes	Yes	2	Stable
1.4	Yes	No	2	Stable

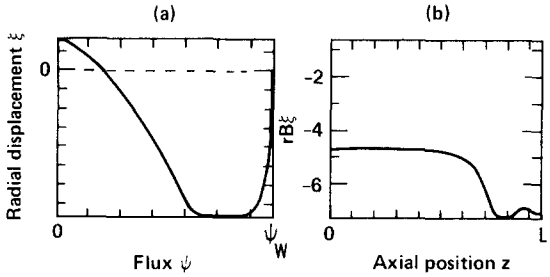

FIG. 7. (a) Radial displacement ξ as a function of flux ψ near the midplane of the center cell and (b) $rB\xi$ as a function of axial position z on an inner flux tube at various times taken from a FLORA initial-value calculation. The center-cell peak beta was $\beta_{\perp c} = 0.5$, and the hot-electron peak beta in the end cell was $\beta_{\perp e} = 0.02$. The equilibrium profiles were much the same as shown in Figs. 1–4.

An important finding revealed by the FLORA calculations is the departure of the computed eigenmodes from the rigid profile assumed in the analysis of Sec. II. We attribute this difference to the radial variation in the strength of the FLR effects in the FLORA calculations. Recall that the rigid-mode stability analysis in Sec. II assumed that FLR effects contributing to ρT were large everywhere. This was essential in transmitting stabilizing effects, e.g., because of hot electrons or a lateral wall, from the outer flux tubes inwards. If the FLR effects are locally large and small somewhere else, then the plasma displacement for an $m = 1$ mode can deviate from rigidity where the FLR is small if this is energetically favorable. Solution of the stability problem then requires the calculation of the radial mode structure as is accomplished in FLORA.

Figure 7 displays radial and axial eigenmode profiles for an $m = 1$ unstable ballooning mode for an equilibrium with peak $\beta_{\perp c} = 0.5$ in the center cell and peak $\beta_{\perp e} = 0.02$ for the hot electrons in the end cell. Because $\Omega_E \equiv 0$ and the pressure profiles were slightly concave on the inner flux tubes (Fig. 3), the characteristic FLR frequencies in Eqs. (6) and (7) were large only on the shoulder of the core-plasma pressure profile beginning two-thirds of the way to the lateral wall. Figure 7(a) indicates that ξ near the center-cell midplane was relatively rigid only on the outer flux tubes where there was strong FLR (except close to the wall where the plasma and the FLR vanished) and that there was a node in the middle of the plasma. The axial mode profile for $rB\xi$ on an inner flux tube [Fig. 7(b)] exhibits ballooning as the mode enters the end cells where the curvature drive is strongest and the FLR is weakest. A flute mode corresponds to $rB\xi = \text{const}$ in z.

IV. DISCUSSION

This paper theoretically demonstrates the stabilizing effects of hot rigid electrons and a nearby conducting wall on high-beta axisymmetric tandem mirror configurations. The stability analysis has been restricted to low-frequency, low-mode-number, incompressible ballooning-interchange modes in long-thin systems. We have analytically extended the rigid-mode stability analysis of Ref. 8 to include hot-electron well digging. The analysis here illustrates the combined influences of a nearby lateral wall and hot electrons on

03 October 2025 23:10:05

stability. This is qualitatively confirmed and extended in our numerical calculations with the FLORA code. Relatively modest hot-electron betas ($\beta_{\perp e} \sim 0.05$) are required to stabilize moderate-beta center-cell plasmas ($\beta_{\perp c} \sim 0.4$), and high-beta wall stabilization is confirmed. Our results lead us to speculate that an MHD-stable axisymmetric configuration might be achieved by using hot-electron rings or disks in the end cells to stabilize transiently a finite-beta center-cell plasma during buildup to a high-beta, wall-stabilized system with no hot electrons in steady state.

ACKNOWLEDGMENTS

We are grateful to H. Gurol, T. B. Kaiser, L. L. LoDestro, W. A. Newcomb, L. D. Pearlstein, D. D. Schnack, and G. W. Shuy for valuable suggestions and assistance in this research.

This work was performed under the auspices of the U. S. Department of Energy by the Lawrence Livermore National Laboratory under Contract No. W-7405-ENG-48 and by Science Applications International Corporation under Massachusetts Institute of Technology Contract No. FC-A-427558.

[1]G. I. Dimov, V. V. Zakaidekov, and M. E. Kishinovskii, Fiz. Plasmy **2**, 597 (1976) [Sov. J. Plasma Phys. **2**, 326 (1976)]; T. K. Fowler and B. G. Logan, Comments Plasma Phys. Controlled Fusion **2**, 167 (1977).

[2]See AIP Document No. PAPS PFLDA-29-1558-336 for 336 pages of *Status of Mirror Fusion Research 1980*, edited by B. I. Cohen. Order by PAPS number and journal reference from American Institute of Physics, Physics Auxiliary Publication Service, 335 East 45th Street, New York, NY 10017. The price is $1.50 for each microfiche (98 pages) or $5.00 for photocopies of up to 30 pages, and $0.15 for each additional page over 30 pages. Airmail additional. Make checks payable to the American Institute of Physics.

[3]T. B. Kaiser and L. D. Pearlstein, Phys. Fluids **26**, 3053 (1983); T. B. Kaiser, W. M. Nevins, and L. D. Pearlstein, *ibid.* **26**, 351 (1983).

[4]D. D. Ryutov and G. V. Stupakov, Fiz. Plasmy **4**, 501 (1978) [Sov. J. Plasma Phys. **4**, 278 (1978)]; R. H. Cohen, Comments Plasma Phys. Controlled Fusion **4**, 157 (1979).

[5]W. B. Kunkel and J. U. Guillory, in *Proceedings of the Seventh International Conference on Ionized Gases*, Belgrade, 1965, edited by B. Perovic and D. Tocsis (Gradjerinska Knjiga, Belgrade, 1965), Vol. II, p. 702; D. Segal, M. Wickham, and N. Rynn, Phys. Fluids **25**, 1485 (1982); A. W. Molvik, R. A. Breun, S. N. Golovato, N. Hershkowitz, B. McVey, R. S. Post, D. Smatlak, and L. Yujiri, *ibid.* **27**, 2711 (1984).

[6]B. Lehnert, Phys. Fluids **9**, 1367 (1966); T. D. Rognlien, J. Appl. Phys. **44**, 3505 (1973); M. Z. Caponi, B. I. Cohen, and R. P. Freis, Phys. Fluids **30**, 1410 (1987).

[7]F. A. Haas and J. A. Wesson, Phys. Fluids **10**, 2245 (1967); D. A. D'Ippolito and J. R. Myra, *ibid.* **27**, 2256 (1984); H. L. Berk, M. N. Rosenbluth, H. V. Wong, and T. M. Autonsen, Jr., *ibid.* **27**, 2705 (1984).

[8]T. B. Kaiser and L. D. Pearlstein, Phys. Fluids **28**, 1003 (1985).

[9]D. B. Nelson and C. L. Hedrick, Nucl. Fusion **19**, 283 (1979).

[10]D. A. D'Ippolito, J. R. Myra, and J. M. Ogden, Plasma Phys. **24**, 707 (1982).

[11]S. I. Kishimoto, Y. Yamamoto, H. Akimune, and T. Suita, J. Phys. Soc. Jpn. **38**, 231 (1975); Y. Yamamoto, S. I. Kishimoto, H. Akimune, and T. Suita, *ibid.* **39**, 795 (1975); J. R. Ferron, N. Hershkowitz, R. A. Breun, S. N. Golovato, and R. Goulding, Phys. Rev. Lett. **51**, 1955 (1983); D. A. D'Ippolito and J. R. Myra, Phys. Fluids **29**, 2596 (1986).

[12]B. I. Cohen, R. P. Freis, and W. A. Newcomb, Phys. Fluids **29**, 1558 (1986).

[13]R. R. Dominguez and H. L. Berk, Phys. Fluids **21**, 827 (1978).

[14]D. E. Baldwin and H. L. Berk, Phys. Fluids **26**, 3595 (1983); H. L. Berk and T. B. Kaiser, *ibid.* **28**, 345 (1985).

[15]K. Tsang, X. S. Lee, B. Hafizi, and T. Antonsen, Phys. Fluids **27**, 2511 (1984); K. T. Tsang and X. S. Lee, Phys. Rev. Lett. **53**, 2094 (1984).

[16]L. L. LoDestro, Phys. Fluids **29**, 2329 (1986).

[17]D. B. Nelson, Phys. Fluids **23**, 1850 (1980); J. W. Van Dam and Y. C. Lee, in *Proceedings of the Workshop on EBT Ring Physics* (Oak Ridge National Laboratory, Oak Ridge, TN, 1979), p. 471.

03 October 2025 23:10:05